

1 **Impact of meteorological conditions on BVOC emission rate from Eastern**
2 **Mediterranean vegetation under drought**

3
4 Qian Li^{1,2}, Gil Lerner², Einat Bar³, Efraim Lewinsohn³, Eran Tas^{2*}

5 ¹ School of Ecology, Hainan University, No 58, Renmin Avenue, Haikou, Hainan province,
6 China

7 ² Institute of Environmental Sciences, The Robert H. Smith Faculty of Agriculture, Food and
8 Environment, The Hebrew University of Jerusalem, P.O. Box 12, Rehovot 7610001, Israel

9 ³ Department of Vegetable Research, Agricultural Research Organization – Newe Ya'ar Center,
10 Israel

11
12
13
14
15 * Correspondence to:

16 Eran Tas, Institute of Environmental Sciences, The Robert H. Smith Faculty of Agriculture, Food
17 and Environment, The Hebrew University of Jerusalem, P.O. Box 12, Rehovot 7610001, Israel
18 eran.tas@mail.huji.ac.il

19 **Abstract**

20 A comprehensive characterization of drought's impact on biogenic volatile organic
21 compounds (BVOC) emissions is essential for understanding atmospheric chemistry under
22 global climate change, with implications for both air quality and climate model simulation.
23 Currently, the effects of drought on BVOC emissions are not well characterized. Our study
24 aims to test: i) whether instantaneous changes in meteorological conditions can serve as a
25 better proxy for drought-related changes in BVOC emission compared to the absolute
26 values of the meteorological parameters, as indicated in a companion article based on
27 BVOC mixing-ratio measurements; ii) the impact of a plant under drought stress receiving
28 a small amount of precipitation on BVOC emission rate, and on the manner in which the
29 emission rate is influenced by meteorological parameters. To address these objectives, we
30 conducted our study during the warm and dry summer conditions of the Eastern
31 Mediterranean region, focusing on the impact of drought on BVOC emissions from natural
32 vegetation. Specifically, we conducted branch-enclosure sampling measurements in Ramat
33 Hanadiv Nature Park, both under natural drought and after irrigation (equivalent to 5.5–7
34 mm precipitation), for six selected branches of *Phillyrea latifolia*, the highest BVOC
35 emitter in this park, in September–October 2020. The samplings were followed by gas
36 chromatography-mass spectrometry analysis for BVOCs identification and flux
37 quantification. The results corroborate the finding that instantaneous changes in
38 meteorological parameters, particularly relative humidity (RH), offer the most accurate
39 proxy for BVOC emission rates under drought, compared to the absolute values of either
40 temperature (T) or RH. However, after irrigation, the correlation of the detected BVOC
41 emission rate with the instantaneous changes in RH became significantly more moderate,

42 or even reversed. Our findings highlight that under drought, the instantaneous changes in
43 RH, and to a lesser extent in T, are the best proxy for the emission rate of monoterpenes
44 (MTs) and sesquiterpenes (SQTs), whereas under moderate drought conditions, T or RH
45 serves as the best proxy for MT and SQT emission rate, respectively. In addition, the
46 detected emission rates of MTs and SQTs increased by 150% and 545%, respectively, after
47 a small amount of irrigation.

48

49 **1 Introduction**

50 Biogenic volatile organic compounds (BVOCs) are released by plants and other organisms
51 to the atmosphere. They play a critical role in both climate change and photochemical air
52 pollution (Cai et al., 2021; Calfapietra et al., 2013; Curci et al., 2009; Guenther, 2013;
53 Kesselmeier and Staudt, 1999; Peñuelas et al., 2009). BVOCs are thought to be emitted by
54 plants as a defense mechanism against biotic and abiotic stresses, such as herbivory and
55 high temperatures (Berg et al., 2013; Blande et al., 2007; Brilli et al., 2009; Peñuelas and
56 Munné-Bosch, 2005). BVOCs may also be involved in plant–plant and plant–animal
57 communication, allowing plants to signal to other organisms about their response to
58 environmental conditions (Baldwin et al., 2006; Filella et al., 2013; Niinemets and Monson,
59 2013).

60 The emission rate and composition of BVOCs can vary widely depending on
61 various factors, such as meteorological conditions, rate of synthesis, and physicochemical
62 properties (Niinemets and Monson, 2013). Climate change is expected to significantly
63 impact BVOC emission rate and composition. As temperature rises, the emission rate of
64 most BVOCs increases in an Arrhenius-type manner (Goldstein et al., 2004; Greenberg et

65 al., 2012; Guenther et al., 1995; Monson et al., 1992; Niinemets et al., 2004; Tingey et al.,
66 1990). On the other hand, drought can have a more complex effect on the emission and
67 composition of BVOCs. Depending on the type of vegetation, the level of drought stress,
68 and additional ambient conditions, the emission of BVOCs can be partially or completely
69 suppressed (Fortunati et al., 2008; Holopainen and Gershenzon, 2010; Llusia et al., 2016;
70 Peñuelas and Staudt, 2010; Schade et al., 1999), or enhanced in a way that has not yet been
71 characterized (Fitzky et al., 2023; Geron et al., 2016; Potosnak et al., 2014).

72 The effect of drought on isoprene emission has been extensively studied, and it was
73 discovered to be postponed relative to, and/or less significant than the effect on
74 photosynthetic rate (Asensio et al., 2007; Brillì et al., 2007; Fortunati et al., 2008; Pegoraro
75 et al., 2006; Ryan et al., 2014). However, whereas under moderate drought stress, isoprene
76 emission may only slightly decrease or increase, it was shown to decrease considerably
77 under severe or prolonged drought stress (Fortunati et al., 2008; Han et al., 2022; Jiang et
78 al., 2018). The impact of drought on the emission of other BVOCs, such as monoterpenes
79 (MTs) and sesquiterpenes (SQTs), has been less studied.

80 The Eastern Mediterranean has a unique climate characterized by a hot and dry
81 summer, making it an ideal location to study the impact of drought on BVOC emissions.
82 The semiarid and arid regions are particularly vulnerable to climate change, and climate
83 simulations predict that the Eastern Mediterranean region will experience more frequent
84 and severe droughts in the future (Giorgi and Lionello, 2008; Lionello, 2012). Research
85 conducted in Israel has investigated the impact of drought on BVOC emissions from a
86 range of local plant species. For example, Llusia et al. (2016) examined the effect of
87 drought on terpene emission from Yatir Forest, a pine forest in the northern Negev. They

88 found that some of the MT and SQT emissions increased under moderate drought
89 conditions but strongly decreased under severe drought conditions. Another measurement
90 by Li et al. (2024), performed in late autumn 2016 in Shibli Forest in northern Israel, found
91 that under severe drought stress, BVOC emissions respond more significantly to the
92 instantaneous changes in meteorological parameters (especially relative humidity [RH])
93 than to the meteorological parameters themselves. These studies suggest that the impact of
94 drought on BVOC emissions is not well-characterized and varies in a complex manner,
95 depending on plant species, BVOC type, and meteorological parameters, such as
96 temperature (T) and RH, as well as the level of drought stress. Hence, more research is
97 needed to better characterize the effect of drought on BVOC emission rates and
98 composition, which can in turn improve air quality and climate modeling.

99 In this study, we use the severe drought conditions during the autumn in the Eastern
100 Mediterranean to study the effect of drought on the emission of BVOCs from natural
101 vegetation. The main specific objectives of this study were to: i) identify whether
102 instantaneous changes in meteorological parameters can serve as a better proxy for BVOC
103 emission rates under drought than their absolute values, and ii) determine the extent to
104 which small precipitation amounts, under drought conditions, can impact BVOC emission
105 rates and the manner in which the emission rate is influenced by meteorological parameters.

106

107 **2 Methods**

108 We used an enclosure-based measurement system to quantify BVOC emissions, allowing
109 for direct measurement of BVOC fluxes at the branch level. The measurements were
110 performed in autumn under the prolonged drought stress conditions typical to this region.

111 BVOC measurements in the Eastern Mediterranean are rare, and to the best of our
112 knowledge, our study is the first to apply direct measurements of BVOC flux from specific
113 branches of natural vegetation in this region. Plants were sampled before and after the
114 application of a small amount of irrigation to study the response of BVOC emissions, under
115 exposure to natural drought conditions, to a small amount of precipitation. This was
116 followed by gas chromatography–mass spectrometry (GC–MS) to identify and quantify
117 the emitted BVOCs. Closed chambers are often used for measurements of BVOCs at the
118 branch level (Duhl et al., 2008). Compared to open-system methods, the enclosure-based
119 system (including a glass cuvette or Tedlar bag) can focus on specific vegetation in a more
120 controlled manner. To investigate the effects of drought on BVOC emission rates and
121 composition, we performed two sets of measurements – before and after irrigation – for
122 comparison. To study the effect of meteorological conditions on BVOC flux, we monitored
123 meteorological parameters inside the bag and at a meteorological station that was 300–600
124 m from the branches.

125

126 *2.1 Sampling site and studied species*

127 The on-site branch measurements were conducted at Ramat Hanadiv Nature Park (32°
128 33' 19.87" N, 34° 56' 50.23" E), 3.6 km from the Eastern Mediterranean seashore and
129 exposed to a typical Eastern Mediterranean climate, with annual precipitation of 640 mm
130 (averaged over the last 5 years, and occurring mainly between November and March). The
131 vegetation at the site is dominated by mixed Mediterranean shrubbery. More details about
132 the site and vegetation can be found in Li et al. (2018) and Dayan et al. (2020). The
133 measurements were conducted at the end of summer/beginning of autumn under drought

134 conditions. No precipitation was recorded for 108 days between 24 May 2020 and the
135 beginning of the study on 9 Sep 2020.

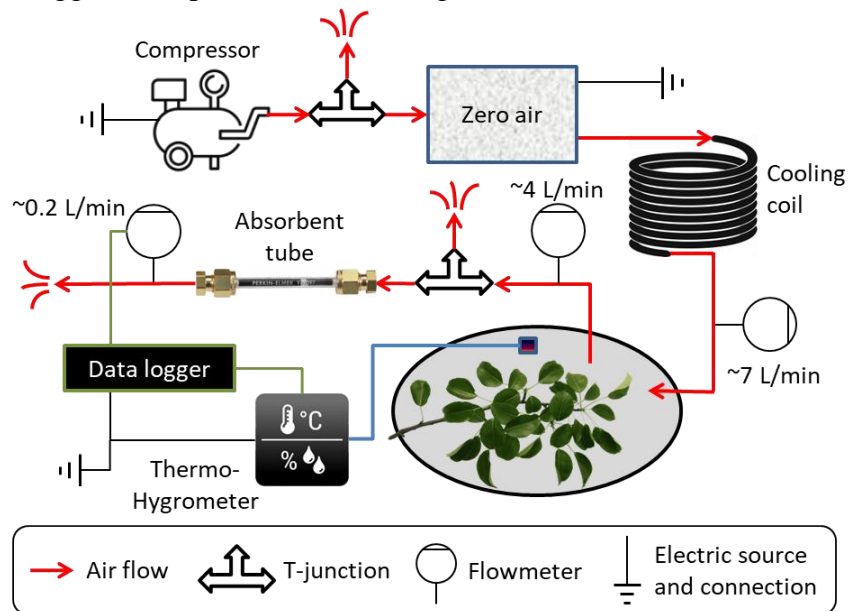
136 *Phillyrea latifolia* (broad-leaved phillyrea), identified as the greatest BVOC-
137 contributing plant species in the Ramat Hanadiv natural park, was sampled. The species is
138 native to the Mediterranean Basin and belongs to the family Oleaceae. In Ramat Hanadiv,
139 it accounts for 7.5% of all vegetation, but up to ~35% of all BVOC emissions, according
140 to the Model of Emissions of Gases and Aerosols from Nature (MEGAN v2.1; Dayan et
141 al., 2020; Guenther et al., 2012; Li et al., 2018). The selected plants were mature and did
142 not show any visible signs of senescence. Sampled branches were shaded, to eliminate the
143 effect of non-natural high temperature in the enclosure system, and measurements were
144 performed at 1.5 to 2 m aboveground.

145

146 ***2.2 Branch-enclosure sampling system and setup***

147 Figure 1 presents a self-made branch-sampling system was used for this study. All tubes
148 and connections are Teflon, while valves and flowmeters are stainless steel. A compressor
149 provides a controllable rate of ambient air flow through an adjustable T-junction valve (to
150 adjust the flow rate) to a zero-air device (Model 1150 dual reactor, Thermo Fisher
151 Scientific, Waltham, MA, USA), which includes a catalytic converter heated to ~350 °C to
152 oxidize carbon monoxide (CO) and hydrocarbons (HC) to carbon dioxide (CO₂) and water
153 (H₂O). From the zero-air device, the air flows through a copper coil to cool it down, and
154 then through a mass flowmeter into a Tedlar bag (CEL Scientific Corporation, Cerritos,
155 CA, USA), at a flow rate of about 7 L min⁻¹ (monitored by flowmeter A), a high enough
156 inflow to produce slight overpressure inside the bag. The inert and light-transparent 10 L

157 Tedlar bag is tied tightly around a tree branch, along with an EL-MOTE-TH temperature
 158 and RH sensor (Lascar Electronics, Whiteparish, Wiltshire, UK). The outlet airflow (~ 4 L
 159 min^{-1} monitored by flowmeter B) is directed to the C2-CAXX-5032 hydrophobic inert-
 160 coated stainless-steel adsorbent tube (CSLR, Markes International, Llantrisant, UK) filled
 161 with a mixture of Tenax TA and Carbograph as adsorbent, at a rate of ~ 0.2 L min^{-1}
 162 (monitored by flowmeter C), regulated by the T-junction valve downstream of flowmeter
 163 B. The flow rate through the adsorbent tube, as well as T and RH were recorded with a
 164 CR1000 data logger (Campbell Scientific, Logan, UT, USA).



165 **Figure 1.** Schematic of the branch-enclosure sampling system. VOCs are removed from the ambient air
 166 before entering a transparent Tedlar bag and an adsorbent tube to monitor BVOC emissions from the enclosed
 167 branch, using a flow-controlled system (see Sect. 2.2).

168

169 **2.3 Analytical quantification of the sampled BVOCs**

170 A Centri™ (Markes International) preconcentration system was used to desorb the tubes
 171 into the cold trap (graphitized carbon trap; used for sampling VOCs of C4/5 to C30/32)
 172 under the following conditions: desorption for 5 min at 280 $^{\circ}\text{C}$ with a trap flow of 30 mL

173 min⁻¹. Desorption of trap was at a rate of 20 °C s⁻¹ to 300 °C into an Agilent GC–MS
174 (7890A/5975C) system (Santa Clara, CA, USA) equipped with a Stabilwax column
175 (Restek, 30 m, 0.25 mm ID capillary column; polyethylene glycol, 0.25 µm film thickness).
176 The general run parameters were as follows: injector, 230 °C; column oven, initial
177 temperature of 45 °C for 5 min, followed by a ramp of 5 °C min⁻¹ to 120 °C, 20 °C min⁻¹
178 to 240 °C final, and 5-min hold with a total run time of 31.5 min; carrier gas, He 32 psi;
179 mass spectrometer ionization energy, 70 eV; m/z, 41 to 300; scan time, 5.4 s. The
180 chromatograms were analyzed using MassHunter Quant Analysis (B.10.00, Agilent
181 Technologies, Santa Clara, CA, USA) software. Compounds were identified by comparing
182 their relative retention indices and mass spectra with those of authentic standards or those
183 found in the literature, supplemented with W10N14 and 2205 GC–MS libraries.

184 We chose to analyze the most abundant BVOC species: *cis*-β-ocimene (E, Z) (MT),
185 and β-caryophyllene, α-humulene, α-farnesene, germacrene-D (SQTs). For calibration,
186 analytical-grade standard solutions (7–12 concentrations) were prepared, ranging in
187 concentrations from 0.25 to 1000 ng mL⁻¹ by diluting known masses of pure chemicals
188 with methanol. The calibration analytes were injected using a GC syringe onto clean
189 sorbent tubes connected to a calibration solution-loading rig (Markes International) at a
190 nitrogen flow of 80 mL min⁻¹ for 5 minutes. The standards for the BVOC species were *cis*-
191 β-ocimene (E, Z) (W353977, Sigma-Aldrich) (MT), and β-caryophyllene (22075-1ML-F,
192 Sigma-Aldrich), α-humulene (PHL83351, Sigma-Aldrich), α-farnesene (Biosynth®
193 Carbosynth Ltd., UK), germacrene-D (Toronto Research Chemicals, Canada) (SQTs),
194 according to the most abundant species (see Sect. 2.4). The sampled solution was mixed
195 with 5 µL of each compound in the solvent. All standard-loaded tubes were prepared in

196 triplicate and results were averaged. The loaded tubes were analyzed under the same
197 conditions used for the other samples. Standard curves of peak area counts vs. VOC mass
198 (μg) were fitted using linear regression analyses; both yielded high regression coefficients
199 ($r^2 \geq 0.99$ in most cases). More details on the calibration are provided in Sect. S1. For the
200 minor MTs and SQTs, the calibration curve of *cis*- β -ocimene (E, Z) and the averaged
201 calibration curve of the four most abundant SQTs were used for a rough estimation of their
202 emission rates.

203

204 ***2.4 Experimental setup***

205 ***2.4.1 Branch sampling, meteorological parameter measurements and flux evaluation***

206 The field measurements were performed from late summer to early autumn – 9 Sep to 27
207 Oct 2020. Samplings were conducted on six selected *Phillyrea latifolia* branches on
208 different bushes. Each branch was measured over two sequential days: 8–9 Sep, 14–15 Sep,
209 22–23 Sep, 12–13 Oct, 19–20 Oct, and 26–27 Oct. The bushes were at least 20 m apart, to
210 enable selective irrigation for individual shrubs. Meteorological parameters were measured
211 at a distance of 300–600 m from the branch measurements. These parameters included T
212 and RH, measured using a Campbell HC2S3 probe; net radiation, measured with a CNR4
213 Kipp & Zonen net radiometer; and wind speed and direction, recorded by a 05103 R.M.
214 Young sensor. Eight 30-min samplings were performed per measurement day. In addition,
215 two reference samplings were performed with full equipment setup, but no branch inside
216 the bag. These reference samplings were performed before and after the eight
217 measurements. On each measurement day, after completing the first sampling for reference,
218 the system and branches were given at least 60 minutes to adapt to the different conditions

219 after placing the branch into the bag and setting up the equipment. At the end of the first
220 measurement day, the sampled branch was removed from the bag and returned after the
221 reference sampling on the second day. Following the 9th sampling on the second
222 measurement day of each two-sequential-day period, the sampled branch was cut and sent
223 to the laboratory for leaf analysis. Leaf wet weight and area were evaluated within 24 h
224 after cutting the branch. All leaves were scanned, and a digital color-based image-
225 processing method was used to identify the total (RGB values: 40–200, 50–200, 30–200)
226 and healthy (RGB values: 40–110, 50–105, 30–80) leaf areas. The leaves were then dried
227 for 72 h at 60 °C, and their net dry weight was recorded.

228 The sampling tubes were kept in a cooler with a temperature below 5 °C after the
229 measurement, and analyzed within 5 days of sampling by GC–MS (see Sect. 2.3). Of the
230 identified species, one MT and four SQT compounds (*cis*- β -ocimene, β -caryophyllene, α -
231 humulene, α -farnesene, and germacrene D) with the highest sampled mass for each of the
232 branches were chosen for quantification by GC–MS (see Sect. 2.3).

233 The emission rate of BVOCs per leaf area, E_A (ng cm⁻² h⁻¹), for a branch was
234 evaluated by the following formula:

$$235 \quad E_A = \left(m \frac{F_{in-B}}{F_{out-T}} \right) / (A \cdot t) \quad (1)$$

236 where m (ng) is the evaluated mass of any BVOC compound inside the tube, F_{in-B} (L min⁻¹)
237 and F_{out-T} (mL min⁻¹) are the flow rate pumped into the bag and the flow rate through
238 the adsorbent tube, respectively, A (cm²) is the total leaf area of the branch, and t (h) is the
239 sampling time.

240 The emission rate of BVOCs per biomass, E_M (ng g⁻² h⁻¹), was evaluated by:

$$241 \quad E_M = \left(m \frac{F_{in-B}}{F_{out-T}} \right) / (M \cdot t) \quad (2)$$

242 where M (g) is the leaf biomass of the branch.

243

244 **2.4.2 Irrigation and soil-water content quantification**

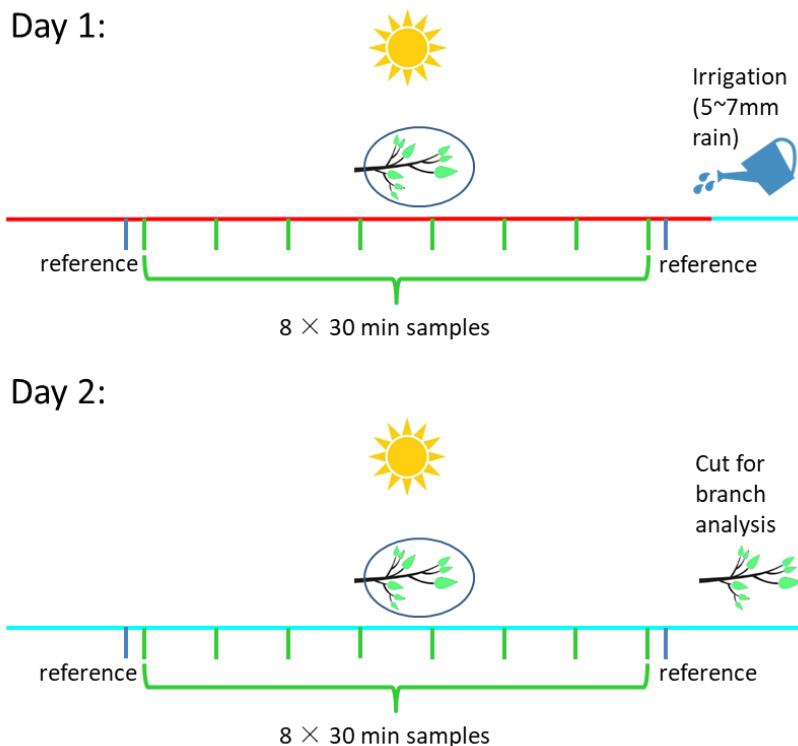
245 Manual irrigation was applied at the end of the first measurement day of each 2-sequential-

246 day measurement period (see Fig. 2). The irrigation amounts were 50–70 L within a radius

247 of 1–2 m from the stem of the plants used for sampling (equivalent to 5.5–7 mm rain). This

248 irrigation served to identify the potential effect of a small precipitation event during a

249 drought period on BVOC emission rate and composition.



250 **Figure 2.** Schematic of the experimental design. Day 1 and Day 2 represent, respectively, the first and

251 second day of each two-sequential-day sampling period for a specific branch. Green and blue bars represent

252 sampling measurements and reference measurements, respectively. The red and cyan lines mark sampling

253 prior to manual irrigation on Day 1 and after manual irrigation, on Day 2, respectively.

254 Ten soil samples were collected at solar noon time within 2 m from the sampled
 255 plant on every experimental day. To evaluate the soil-water content, soil samples were
 256 weighed on the day of collection, and weighed again after drying them in an oven at 105 °C
 257 for 24 h. The following formula was used to calculate the soil-water content:

$$258 \quad w = \frac{M_{tot} - M_{dry}}{M_{dry}} \times 100\% \quad (3)$$

259 where w (g/g) is the soil gravimetric water content and M_{tot} (g) and M_{dry} (g) are the total
 260 and dried soil mass, respectively.

261

262 ***2.4.3 Correlation between BVOC emission rate and temporal changes in RH and T***

263 To test the effect of instantaneous changes in RH and T on the emission rate of the sampled
 264 BVOCs, we studied the correlation between the temporal changes in both ambient air RH
 265 and T with the BVOC emission rate during the sampling. BVOC sampling length was 30
 266 min, with a gap of 1 h between each sampling. To account for instantaneous changes in
 267 RH and T we introduce δ_{RH} and δ_T , respectively. δ_{RH} is defined as follows:

$$268 \quad \delta_{RH} = \sum_{i=1}^n \left(\frac{RH_{i+1}}{RH_i} - 1 \right) \quad (4)$$

269 where i is the 10 min time step according to the available measurement frequency, and n
 270 is the number of time steps.

271 δ_T is defined in the same manner as follows:

$$272 \quad \delta_T = \sum_{i=1}^n \left(\frac{T_{i+1}}{T_i} - 1 \right) \quad (5)$$

273 The correlations between δ_{RH} , δ_T and the BVOC fluxes for all samples were tested
 274 for different values of n . In a preliminary test, it was found that the highest average
 275 correlations of δ_{RH} and δ_T with BVOC emission rate were obtained when $n = 9$.
 276 Accordingly, the calculation duration of δ_{RH} and δ_T began 60 min before each 30 min

277 BVOC emission rate sampling. This finding is consistent with a similar analysis conducted
278 by Li et al. (2024). Similarly, the correlation between δ_{RH} and δ_T and BVOC emission rate
279 in that study applied δ_{RH} and δ_T which were calculated for 90 min cycles, while the
280 beginning of each cycle was 60 min prior to the beginning of each compatible 30 min
281 BVOC sampling.

282

283 ***2.4.4 Afternoon emission trend (AET) analysis***

284 Under drought conditions, the increased stomatal resistance can largely reduce the BVOC
285 emission rate (see Sect. 1). Accordingly, it was found that the BVOC mixing ratio tends to
286 reach a minimum around noontime when RH tends to reach its daily minimum and stomatal
287 conductance is limited (Nobel, 1999), and then gradually increase in the afternoon (Li et
288 al., 2024). Our observations indicated a clear increase in BVOC emission rates during the
289 afternoon for the days before the irrigation. On those days, no clear decrease in BVOC
290 emission was observed before noon; instead, the BVOCs generally exhibited lower
291 emission rates. Here we introduce a method for quantifying the trend of emission rate right
292 after the mid-day minimum, which applies the afternoon emission trend (AET) index:

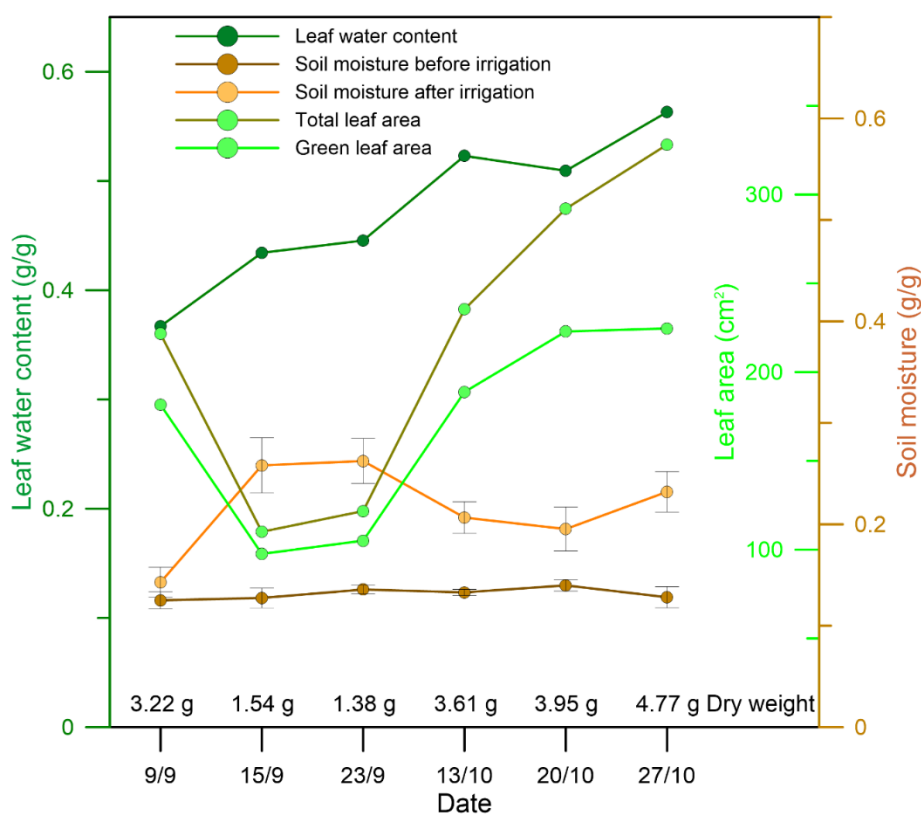
$$293 \quad \text{AET} = \sum_{i=1}^n \left(\frac{E_{i+1}}{E_i} - 1 \right) \quad (6)$$

294 where E_i is the emission rate of the i_{th} sample, while $i = 1$ indicates the minimum value
295 around noontime, between 12:00–14:00 h. Hence, the AET indicates the trend and
296 magnitude of the emission in the afternoon of any measurement day.

297 **3 Results and discussion**

298 **3.1 Analysis of branch leaves**

299 Figure 3 shows the total leaf area (cm²), green leaf area (cm²), leaf water content, and soil
300 moisture before and after irrigation of each sampling branch. Leaf green area ranged from
301 68% to 89% of the total leaf area. Soil moisture ranged from 12.5% to 14.0% before
302 irrigation and from 14.3% to 26.2% after irrigation. Interestingly, the leaf water content
303 after irrigation increased gradually during the experimental period, indicating that the
304 capacity for water uptake from the soil increases with drought prolongation.



305 **Figure 3.** Properties of the sampled branch leaves and soil moisture within a radius of 1 m from the stem of
306 the sampling plant. Presented leaf property values are averages over all sampled branch leaves.

307 **3.2 Emission rates of MTs and SQTs**

308 Whereas previous branch enclosure studies focused primarily on isoprene emissions
309 (Genard-Zielinski et al., 2015; Genard-Zielinski et al., 2018; Saunier et al., 2017), our
310 measurements did not detect large amounts of isoprene emissions from the selected
311 *Phillyrea latifolia*, in line with previous studies showing that some plant types do not emit
312 notable amounts of isoprene (Aydin et al., 2014; Bracho-Nunez et al., 2013). Our analysis
313 focused on the MTs and SQTs detected in our observations, as described in the following
314 section.

315

316 **3.2.1 MTs**

317 On all 10 sampling days for which MTs were identified, the 5 days prior to irrigation were
318 under drought conditions (i.e., more than 100 days after the last precipitation event), and 5
319 days were under irrigation conditions on the same branches (see Sect. 2.4.2). The branch
320 which was sampled on Sep 14–15 did not show any detectable MT emission. The diurnal
321 emission fluxes of MTs from the branches are shown in Fig. 4.

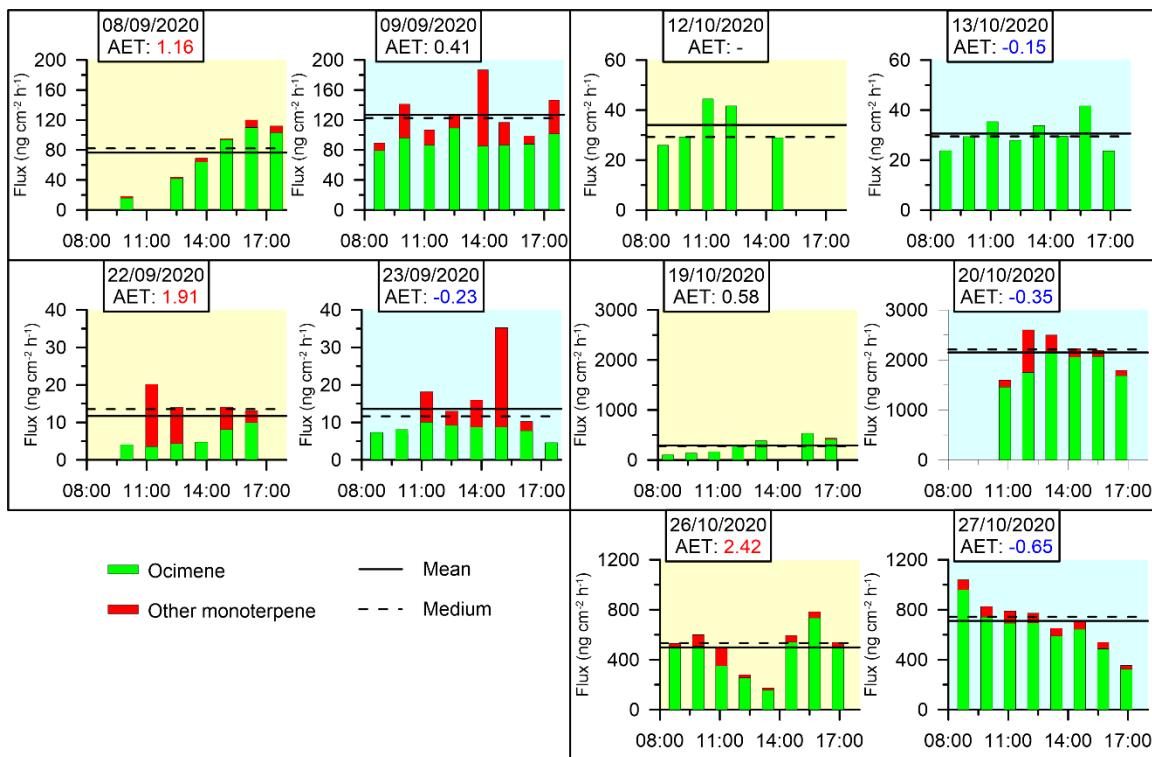
322 The daily average emission rate of MTs over all sampling days ranged from 11.7–
323 2151.4 ng cm⁻² h⁻¹ (0.89–121.5 μg g⁻¹ h⁻¹), with *cis*-β-ocimene being the most abundant for
324 each of the sampling branches, averaging at 88% of all detected MTs. These MT emission
325 rates are similar to previous branch enclosure studies, which were conducted
326 predominantly between May and October under Western Mediterranean conditions, where
327 they ranged from 0 to approximately 140 μg g⁻¹ h⁻¹ (Bracho-Nunez et al., 2013; Llusia and
328 Peñuelas, 2000; Núñez et al., 2002; Owen et al., 1997; Owen and Hewitt, 2000; Staudt et
329 al., 2001; Street et al., 1997). Less information is available on the emission rates of MTs in

330 the Eastern Mediterranean. Aydin et al. (2014) used a branch enclosure system to detect
331 emission rates ranging from 0.0047 to 14.2 $\mu\text{g g}^{-1} \text{h}^{-1}$ in 14 different forested areas in
332 Turkey. Seco et al. (2017) quantified MT emissions using eddy covariance method in pine
333 forests in Israel, studying a semiarid site (Yatir) and a Mediterranean sub-humid site (Birya)
334 in the spring. Emission fluxes were found to average at 40 $\text{ng cm}^{-2} \text{h}^{-1}$ (Yatir) and 100 ng
335 $\text{cm}^{-2} \text{h}^{-1}$ (Birya), with peak values of 100 (Yatir) and 190 (Birya) $\text{ng cm}^{-2} \text{h}^{-1}$, while the
336 daytime standardized MT emission capacities were similar across both sites.

337 In our study, MT emissions under drought conditions ranged from 11.7 $\text{ng cm}^{-2} \text{h}^{-1}$
338 to 499.0 $\text{ng cm}^{-2} \text{h}^{-1}$, which is somewhat higher than other values reported in the Eastern
339 Mediterranean. It is important to note that differences in emission rates between our study
340 and the previously reported values in this region might be attributed to the different
341 measurement methodologies employed. Following irrigation, the mean daily MT emission
342 rates increased in four out of the five investigated branches, and ranged from 13.6 ng cm^{-2}
343 h^{-1} to 2151.4 $\text{ng cm}^{-2} \text{h}^{-1}$. This reflects an average 150% increase for all sampling days in
344 the range of emission rates following irrigation, indicating that even a small amount of
345 water during a period of drought stress can significantly influence MT emissions. This
346 effect may be related to the dramatic increase in stomatal conductance, due to the increase
347 in water availability following irrigation (Medrano et al., 2002; Miyashita et al., 2005;
348 Vilagrosa et al., 2003). It is also observed that on some of the sampling days, the
349 composition of MTs tends to become more diverse after irrigation compared to before
350 irrigation, warranting further study.

351 AET (Sect. 2.4.4) values specified in figures 4 and 5 reinforced the significant effect of
352 small irrigation amounts on BVOC emission rates under drought, considering that on

353 drought days, AETs were high and positive, whereas after irrigation, AETs became
 354 moderate or negative. This observation is consistent with previous studies showing that the
 355 emission of BVOCs can be affected by the vegetation's stomatal activity, which tends to
 356 be lower around noontime during drought stress (Li et al., 2023; Seco et al., 2017). Stomatal
 357 resistance is typically two orders of magnitude larger than cuticular resistance (Nobel, 1999)
 358 and therefore, the midday minimum and the following increase in MT emissions under
 359 drought conditions may be mostly due to stomatal resistance, which can limit the exchange
 360 of gases between the plant and the atmosphere. In other words, the increased emission of
 361 MTs after irrigation may be due to reopening of the stomata, which allows for the release
 362 of VOCs.



363 **Figure 4** Branches' diurnal MT emission fluxes. No MTs were detected for the branch sampled on 14–15
 364 Sep. Yellow and blue shading indicate the days before and after irrigation, respectively (see Sect. 2.4.2).
 365 Horizontal solid and dashed lines are daytime mean and median fluxes of MTs, respectively. AET values
 366 (see Sect. 2.4.4) are marked in red and blue when they are larger than 1 or negative, respectively.

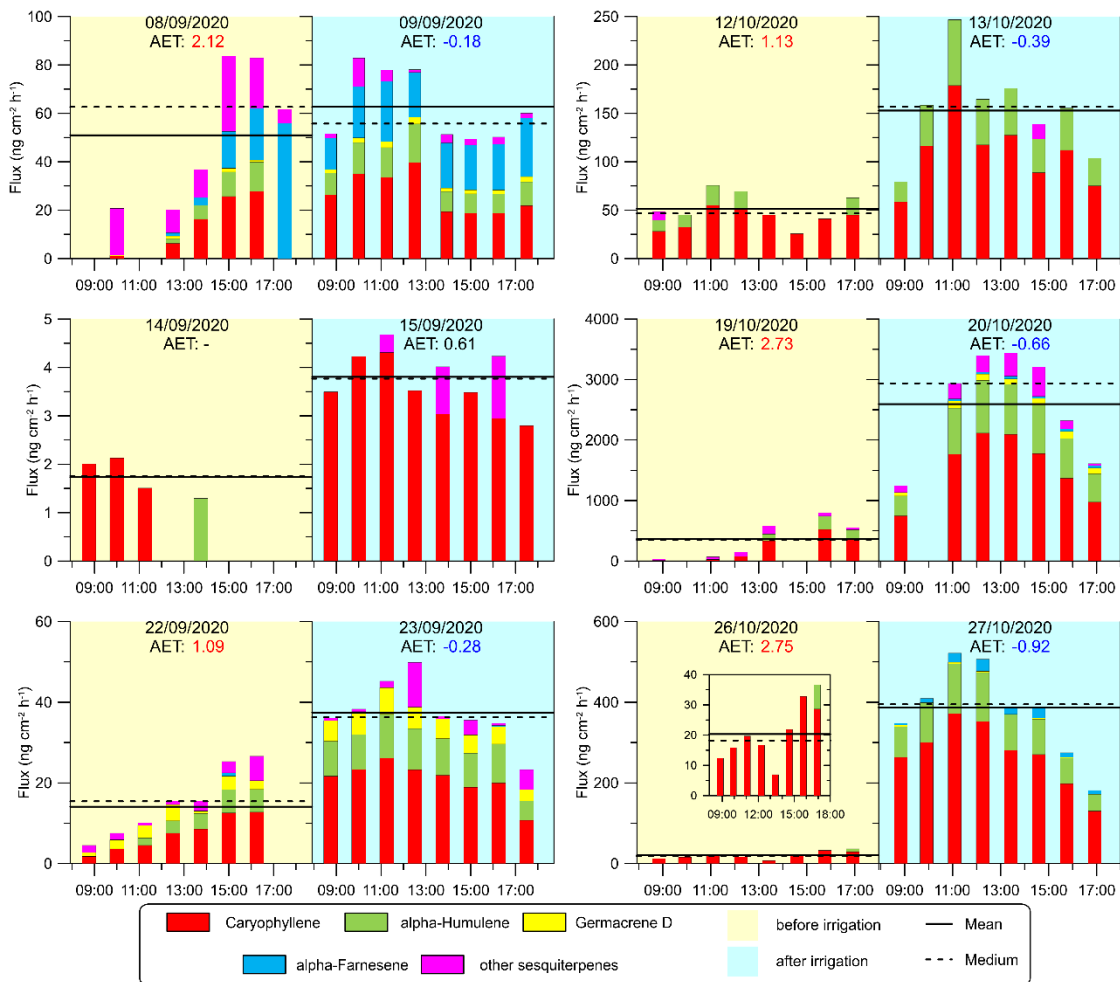
367 3.2.2 SQTs

368 Figure 5 shows the emission fluxes of SQTs for the branches under drought and irrigation
369 conditions. The four most abundant detected SQTs for each of the sampled branches were
370 β -caryophyllene, α -humulene, germacrene D, and α -farnesene. These compounds
371 comprised 90% of all detected SQTs, from all the branches together. The daily average
372 emission rate of SQTs ranged from 1.7–2595.7 ng cm⁻² h⁻¹ (0.11–146.6 μ g g⁻¹ h⁻¹). In
373 contrast to MTs, few studies provide branch enclosure measurements for SQTs. Notably,
374 our study found significantly higher emission rates than previous research conducted
375 between June and October under Eastern Mediterranean conditions, where rates ranged
376 from 0.0011 to 0.63 μ g g⁻¹ h⁻¹ (Aydin et al., 2014; Bracho-Nunez et al., 2013). The emission
377 fluxes of the SQTs were overall comparable to those of the MTs, which is a notable finding,
378 considering that SQT emission rates are frequently around a quarter of the MT flux
379 (Saunders et al., 2003; Sindelarova et al., 2014). The finding of relatively high SQT
380 emission rates appears to be in line with the findings of Li et al. (2023), who reported
381 relatively high mixing ratios of SQTs (33.6 times higher than isoprene, and 18.9 times
382 higher than MTs) under drought conditions in the same region.

383 Furthermore, we found that the increase in SQT emission flux following irrigation
384 (by 545% on average) was more significant than that of the MTs (by 150% on average).
385 This suggests that the response of SQT emissions to water availability is stronger than that
386 of MTs, which could be related to the chemical properties and physiological functions of
387 SQTs in plants. Bonn et al. (2019) found that a sharp increase in SQT emission occurs
388 close to the wilting point to protect the plant against oxidative damage, as also supported
389 by Caser et al. (2019). The latter found that drought can induce the SQT-synthesis

390 mechanism. The strong increase in SQT emission after irrigation in our study further
 391 supports the notion that enhanced synthesis of SQTs occurs shortly after the release of
 392 drought stress. In addition, the SQTs composition, like MTs composition, was observed to
 393 be more diverse after irrigation in most cases, warranting further study.

394



395 **Figure. 5** Diurnal SQT emission fluxes from the sampled branches. Column colors represent the emission
 396 fluxes of four types of SQTs, and the magenta section of the columns refers to other SQTs. Yellow and
 397 blue shading indicate the days before and after irrigation, respectively (see Sect. 2.4.2). Horizontal solid
 398 and dashed lines are daytime mean and median SQT flux rates, respectively. AET values (see Sect. 2.4.4)
 399 are marked in red and blue when they are larger than 1 or negative, respectively. To better present the trend
 400 on 26 Oct, a smaller figure with a smaller scale is added.

401 Interestingly, the high SQT emission rates found in this study are consistent with
402 the findings of a previous study conducted in the same area (Li et. al., 2023), which also
403 reported higher emission fluxes of SQTs compared to other studies. This suggests that there
404 may be a unique level of drought or plant characteristics that contribute to the high emission
405 fluxes of SQTs in this region.

406

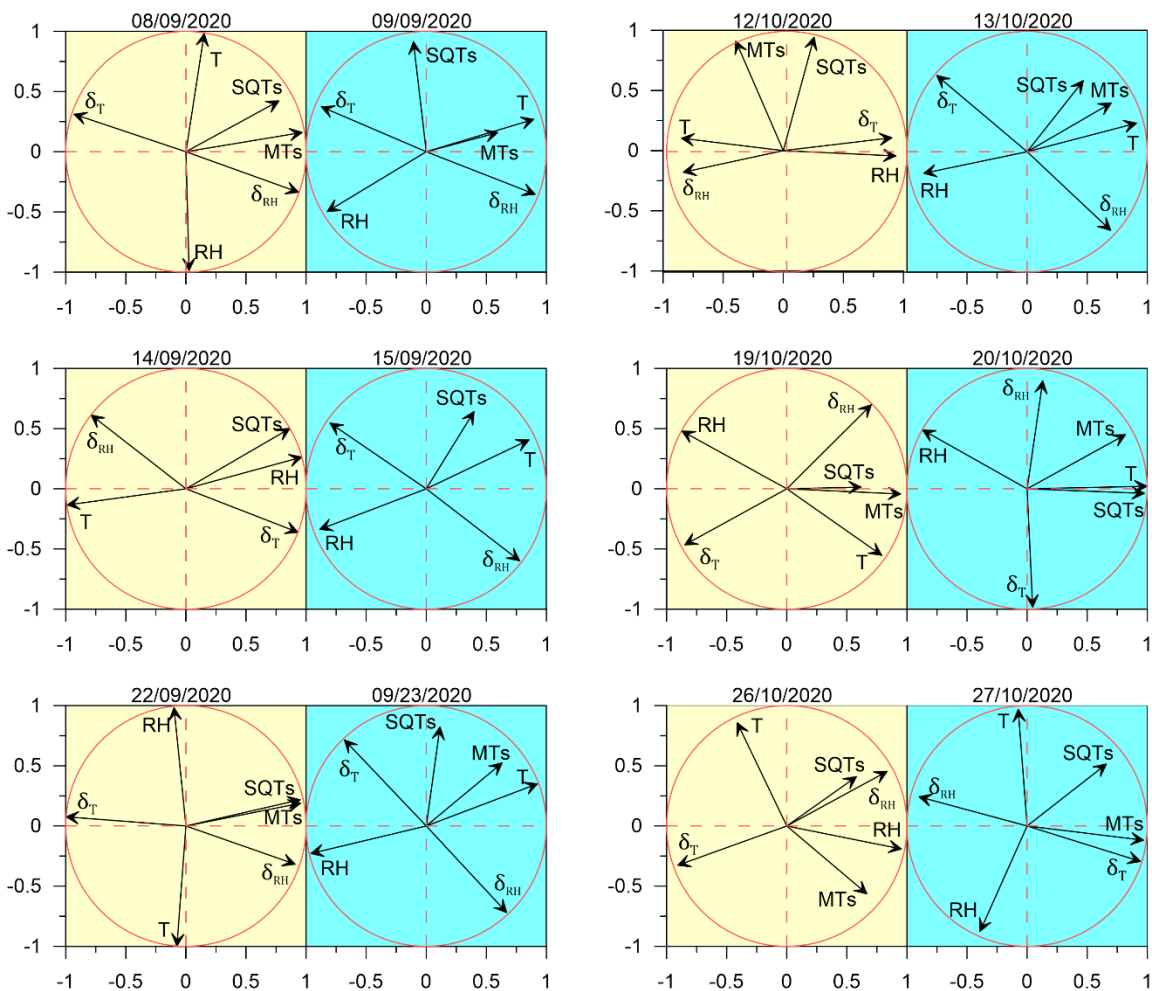
407 ***3.3 The impact of meteorological parameters on MT and SQT emission rates under*** 408 ***drought condition***

409 The effect of meteorological conditions on BVOC emission rate under drought conditions
410 is complex and depends on many factors, including vegetation type, BVOC type, and
411 ambient stress. In the Eastern Mediterranean region, Li et al. (2023) found that under
412 drought, the best proxy for BVOC emission is the instantaneous temporal change in RH;
413 temporal changes in T were also better correlated with BVOC mixing ratio than absolute
414 values of T. Here, we examined the impact of instantaneous changes in ambient air RH and
415 $T - \delta_{RH}$ and δ_T , respectively (see Sect. 2.4.3), as well as of ambient air T and RH on the
416 BVOC emission rate. Due to the large variation in BVOC emissions across different
417 branches, the r values were calculated separately for each branch and each sampling day.
418 Figure 6 presents a principal component analysis (PCA) for the correlation of both δ_{RH} and
419 δ_T with the BVOC emission rates. Before irrigation, when the plants were under drought,
420 on 8 Sep, 22 Sep, 19 Oct, and 26 Oct, the emission rates of the measured BVOC (including
421 both MTs and SQTs) were better correlated with δ_{RH} and δ_T (average Pearson's value (r)
422 of 0.56 and -0.61, respectively) than with RH and T (r of -0.22 and 0.29, respectively).
423 Exceptional are 14 Sep and 12 Oct, also sampled under drought conditions: on 14 Sep, the

424 SQT emissions showed the best correlation with RH ($r = 0.97$); on 12 Oct, the emission
425 rates of BVOCs tended not to correlate with any of the tested meteorological parameters
426 because of a strong correlation of T and δ_{RH} ($r = -0.98$).

427 When focusing only on the days after irrigation, except for 27 Oct, the BVOC
428 emissions were better correlated with T (averaging r values across all relevant days, $r =$
429 0.52) than with any other parameter. Interestingly, on 27 Oct, the SQTs tended to correlate
430 with RH (-0.58), while the MT emission was better correlated with δ_T (0.94). The PCA
431 results show some similarities between the different sampled branches, in their stronger
432 response to δ_{RH} than to the other tested meteorological parameters and their almost
433 complete lack of correlation with T when under drought conditions. However, after
434 irrigation, all BVOC emission rates were highly responsive to T, more than to any other
435 parameter, reflecting the well-known Arrhenius-type increase for BVOC emission with
436 temperature, as mentioned in Sect. 1.

437 Table 1 summarizes the correlation coefficients between the emission rates of
438 SQTs/MTs and RH, T, δ_{RH} , and δ_T , both before and after irrigation. Considering the
439 significant variability in the emission rates of SQTs and MTs across different branches, the
440 r values presented in the table are averages calculated from individual branch-level r values,
441 separately before and after irrigation. Li et al. (2023) showed that under drought conditions,
442 the temporal gradient of meteorological parameters in general was more strongly correlated
443 with BVOC emission rates – not only for RH, but also for T and vapor-pressure deficit.
444 Before irrigation, both SQT and MT emission rates were more strongly correlated with δ_{RH}
445 and δ_T than with RH and T. However, after irrigation, the r values for the correlations with
446 δ_{RH} and δ_T were dramatically weakened. Moreover, following irrigation, the correlations



447 **Figure. 6** PCA analysis for the response of SQTs and MTs to meteorological parameters. The results are

448 presented for SQTs, MTs, T, RH, δ_T , and δ_{RH} , individually for each measurement day. The yellow and
 449 blue shaded areas refer to the day before and after irrigation, respectively.

450

451 with T and RH for both MTs and SQTs were notably stronger than before the irrigation.

452 This indicates that under drought, the temporal gradients in T and RH have a stronger

453 impact on BVOC emissions than the absolute value of T and RH, in agreement with

454 findings by Li et al. (2023). Here, we demonstrate that even a relatively minor precipitation

455 event leads to T becoming the dominant factor in the BVOC emission rate, as expected

456 under non-drought conditions. Interestingly, after irrigation, the highest r value for MTs

457 was with T, but for SQTs, it was with RH.

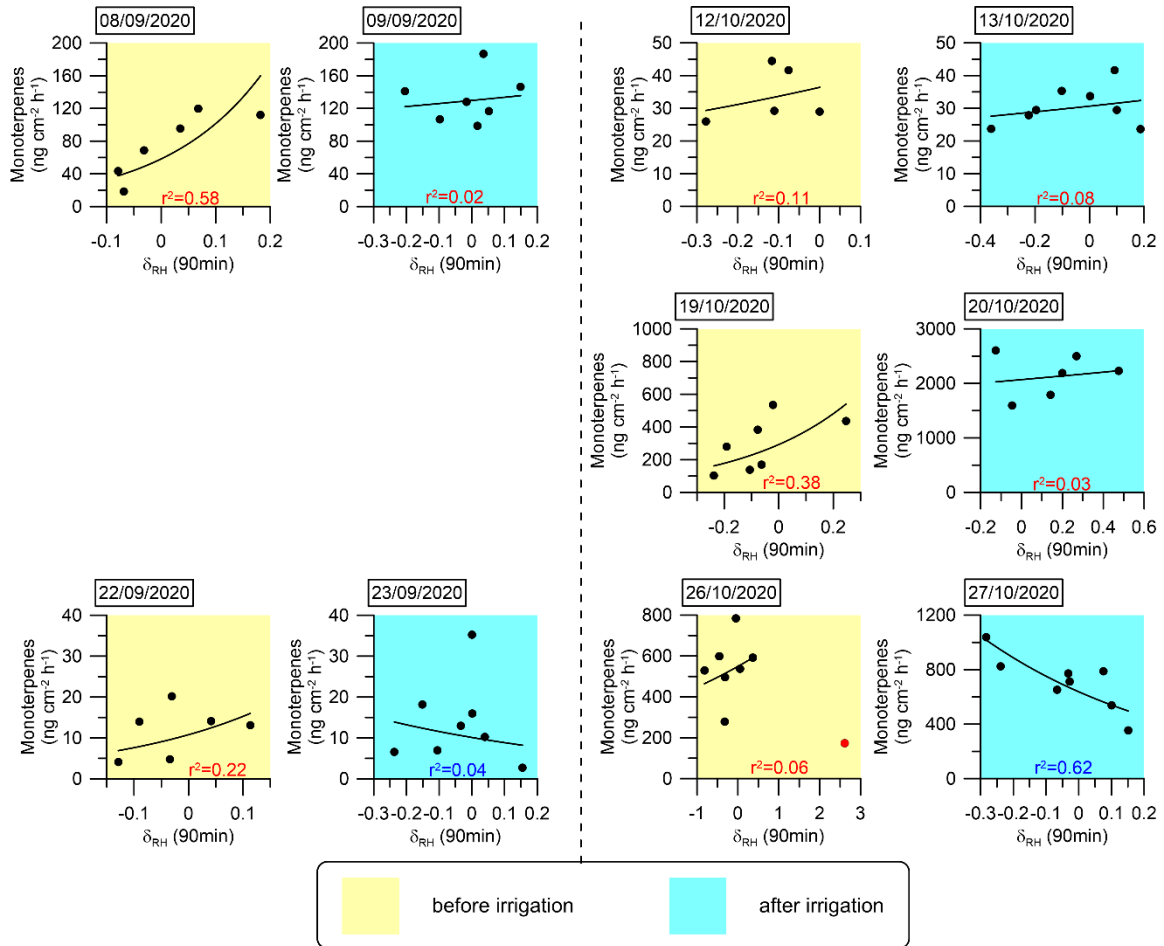
458 **Table 1.** Correlation between the emission rates of MTs and SQTs and the examined meteorological
 459 parameters. Presented are the Pearson's r values for the correlation between MT/SQT emission rate and RH,
 460 T, δ_{RH} , and δ_T (green shading for SQT emissions and lavender shading for MT emissions). The values are
 461 the average of r values across multiple individual branches. Blue and red shading indicates positive and
 462 negative correlation, respectively, and the darkness of the color indicates their values. The P -values for the
 463 correlation are shown in brackets.

Pearson's r value					
SQT	before irrigation	after irrigation	MT	before irrigation	after irrigation
vs RH	-0.22 (0.00)	-0.46 (0.00)	vs RH	-0.18 (0.11)	-0.44 (0.04)
vs T	0.33 (0.02)	0.42 (0.00)	vs T	0.20 (0.02)	0.46 (0.01)
vs δ_{RH}	0.53 (0.02)	-0.11 (0.00)	vs δ_{RH}	0.54 (0.01)	0.00 (0.00)
vs δ_T	-0.50 (0.02)	0.13 (0.00)	vs δ_T	-0.48 (0.01)	0.03 (0.00)

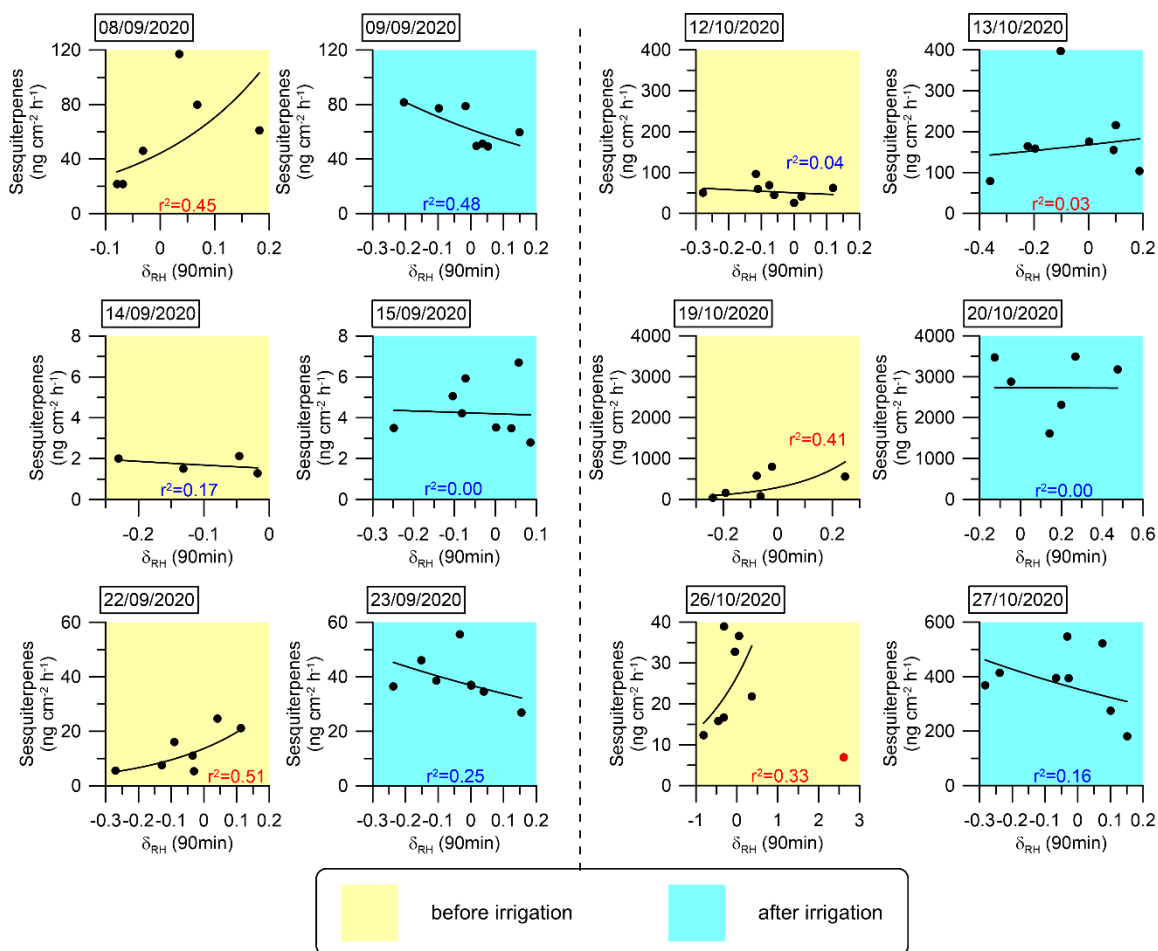
464

465 The analysis presented in Fig. 6 and Table 1 reinforces the finding that
 466 instantaneous changes in meteorological parameters, particularly δ_{RH} , serve as a better
 467 proxy for BVOC emission rate under drought conditions. This finding suggests that
 468 modeling BVOC emission rates under drought conditions can rely on δ_{RH} . In light of this
 469 insight, we investigated the mathematical connection between δ_{RH} and the emission rates
 470 of the MT and SQT fluxes. Exponential fitting corresponded with a relatively strong
 471 correlation between these emission rates and δ_{RH} . Other fitting types used to test this
 472 relationship are presented in Sect. S2. Figures 7 and 8 depict the exponential fitting curves
 473 for MTs and SQTs, respectively. These curves are presented separately for each branch
 474 and individually for drought and post-irrigation conditions. The r^2 for MTs with δ_{RH} ranged
 475 from 0.06 to 0.58 ($r = 0.24$ – 0.76 , average 0.48) under drought, whereas following irrigation,

476 the corresponding correlations ranged from 0.02 to 0.62 ($r = -0.78$ – 0.28 , average -0.08).
 477 For SQTs, the corresponding r^2 values were somewhat higher, ranging from 0.04 to 0.51 (r
 478 $= -0.41$ – 0.67 , average $+0.33$) and 0.00 to 0.48 ($r = -0.69$ – 0.17 , average -0.24), under
 479 drought and following irrigation, respectively.



480 **Figure. 7** Daily correlations between MT emission fluxes and δ_{RH} . An exponential fitting function was used
 481 to fit the curves. The coefficient of determination (r^2) for each day is marked in red or blue when the
 482 correlation is positive or negative, respectively.



483 **Figure. 8** Daily correlations between SQT emission fluxes and δ_{RH} . An exponential fitting function was used
 484 to fit the curves. The coefficient of determination (r^2) for each day is marked in red or blue when the
 485 correlation is positive or negative, respectively. The sample at 12:10 h on 26 Oct 2020 (marked in red) was
 486 not considered in the fitting curve for that day, because an extremely sharp increase in RH (from 10 to 31%)
 487 occurred within 10 min, which we considered an outlier.

488
 489 Overall, these results suggest that while δ_{RH} is likely a better proxy for MT and
 490 SQT emission rates (see Table 1 and Sect. S3), the correlation of δ_{RH} with these BVOCs
 491 appears to be too weak to accurately predict their emission rates using δ_{RH} values in
 492 atmospheric modeling. Additional study is needed before δ_{RH} can effectively serve as a
 493 parameter for modeling BVOC emission rates.

494 Following irrigation, the correlations between the emission flux rates and δ_{RH}
495 became more moderate (4 cases out of 11) or even negative (5 cases out of 11). This further
496 demonstrates the high sensitivity of δ_{RH} 's effect on BVOC emissions to changes in water
497 availability. Further research is required to examine the physiological and biochemical
498 processes underlying the sensitivity of BVOC emission rates to δ_{RH} .

499

500 **4 Summary and conclusions**

501 We investigated BVOC emission rates from branches of *Phillyrea latifolia* under both
502 drought and minor irrigation conditions in the Eastern Mediterranean region, with the aim
503 of assessing the influence of low precipitation levels and meteorological parameters on MT
504 and SQT emission rates during drought stress. We found that leaf water content increases
505 gradually under prolonged periods of drought, indicating the plant's enhanced capacity for
506 water uptake under more severe drought conditions. The highest emission rate among all
507 detected MTs was of *cis*- β -ocimene, and among the detected SQTs, β -caryophyllene, α -
508 humulene, germacrene D, and α -farnesene. Both the MT and SQT emission rates were
509 significantly influenced by the availability of soil water. In response to irrigation, the MT
510 and SQT emission rates increased by 150% and 545%, respectively, indicating that even a
511 small amount of water (equivalent to 5.5–7 mm precipitation) can significantly impact their
512 emission rates.

513 This study highlights the complex way in which meteorological conditions affect
514 BVOC emissions under drought conditions. In line with Li et al.'s (2023) findings, under
515 drought, the instantaneous change of relative humidity, δ_{RH} was the best proxy for BVOC
516 emission rates, as its correlation with MTs and SQTs emission rate ($r = 0.54$ and 0.53 ,
517 respectively) was the strongest among all tested meteorological parameters. However, after

518 a small amount of irrigation (equivalent to 5.5–7 mm precipitation), no correlation was
519 observed between δ_{RH} and MT emission rate, whereas a negative correlation with δ_{RH} was
520 observed for SQT emission rate. The increase in soil water availability led to T (for MTs)
521 or RH (for SQTs) becoming the dominant meteorological parameter affecting BVOC
522 emission rate, making them the best proxies for BVOC emission rates among all tested
523 meteorological parameters. This indicates that changes in water availability can
524 dramatically alter the manner in which BVOC emissions respond to meteorological
525 conditions.

526 Hence, according to the conditions used in this study, under more severe drought,
527 δ_{RH} can serve as the best proxy for BVOC emission rate, whereas under more moderate
528 drought, either T or RH is the best proxy for BVOCs, in agreement with previous findings
529 presented in the companion paper by (Li et al., 2023). Our findings indicate that even a
530 small amount of precipitation can lead to a transition from a drought to non-drought regime
531 in terms of BVOC emission rates and the manner in which they respond to meteorological
532 conditions.

533

534 **Author contribution.** ET designed the experiments, QL and GL carried out the field
535 measurements, QL performed the data acquisition. QL performed the analytical analysis
536 together with EB and EL. QL and ET led the data analyses with contributions from all co-
537 authors. QL and ET prepared the manuscript with contributions from EB.

538

539 **Competing interests.** The authors declare that they have no conflict of interest.

540 **Acknowledgements**

541 This study was supported by the Israel Science Foundation, Grant Nos. 1787/15 and
542 543/22. Eran Tas holds the Joseph H. and Belle R. Braun Senior Lectureship in Agriculture.

543

544 **References**

- 545 Asensio D., Peñuelas J., Llusià J., Ogaya R., Filella I., 2007. Interannual and interseasonal soil CO₂
546 efflux and VOC exchange rates in a Mediterranean holm oak forest in response to
547 experimental drought. *Soil Biology and Biochemistry* 39(10),2471–2484.
548 <https://doi.org/10.1016/j.soilbio.2007.04.019>.
- 549 Aydin Y.M., Yaman B., Koca H., Dasdemir O., Kara M., Altioek H., Dumanoglu Y., Bayram A., Tolunay
550 D., Odabasi M., Elbir T., 2014. Biogenic volatile organic compound (BVOC) emissions from
551 forested areas in Turkey: Determination of specific emission rates for thirty-one tree species.
552 *The Science of the total environment* 490,239–253.
553 <https://doi.org/10.1016/j.scitotenv.2014.04.132>.
- 554 Baldwin I.T., Halitschke R., Paschold A., Dahl C.C. von, Preston C.A., 2006. Volatile signaling in
555 plant-plant interactions: "talking trees" in the genomics era. *Science (New York, N.Y.)*
556 311(5762),812–815. <https://doi.org/10.1126/science.1118446>.
- 557 Berg A.R., Heald C.L., Huff Hartz K.E., Hallar A.G., Meddens A.J.H., Hicke J.A., Lamarque J.-F., Tilmes
558 S., 2013. The impact of bark beetle infestations on monoterpene emissions and secondary
559 organic aerosol formation in western North America. *Atmos. Chem. Phys.* 13(6),3149–3161.
560 <https://doi.org/10.5194/acp-13-3149-2013>.
- 561 Blande J.D., Tiiva P., OKSANEN E., Holopainen J.K., 2007. Emission of herbivore-induced volatile
562 terpenoids from two hybrid aspen (*Populus tremula* × *tremuloides*) clones under ambient and
563 elevated ozone concentrations in the field. *Glob Change Biol* 13(12),2538–2550.
564 <https://doi.org/10.1111/j.1365-2486.2007.01453.x>.
- 565 Bonn B., Magh R.-K., Rombach J., Kreuzwieser J., 2019. Biogenic isoprenoid emissions under
566 drought stress: Different responses for isoprene and terpenes. *Biogeosciences* 16(23),4627–
567 4645. <https://doi.org/10.5194/bg-16-4627-2019>.
- 568 Bracho-Nunez A., Knothe N.M., Welter S., Staudt M., Costa W.R., Liberato M.A.R., Piedade M.T.F.,
569 Kesselmeier J., 2013. Leaf level emissions of volatile organic compounds (VOC) from some
570 Amazonian and Mediterranean plants. *Biogeosciences* 10(9),5855–5873.
571 <https://doi.org/10.5194/bg-10-5855-2013>.
- 572 Brilli F., Barta C., Fortunati A., Lerdau M., Loreto F., Centritto M., 2007. Response of isoprene
573 emission and carbon metabolism to drought in white poplar (*Populus alba*) saplings. *New*
574 *Phytol* 175(2),244–254. <https://doi.org/10.1111/j.1469-8137.2007.02094.x>.
- 575 Brilli F., Ciccioli P., Frattoni M., Prestinini M., Spanedda A.F., Loreto F., 2009. Constitutive and
576 herbivore-induced monoterpenes emitted by *Populus x euroamericana* leaves are key

577 volatiles that orient *Chrysomela populi* beetles. *Plant, cell & environment* 32(5),542–552.
578 <https://doi.org/10.1111/j.1365-3040.2009.01948.x>.

579 Cai M., An C., Guy C., 2021. A scientometric analysis and review of biogenic volatile organic
580 compound emissions: Research hotspots, new frontiers, and environmental implications.
581 *Renewable and Sustainable Energy Reviews* 149(13),111317.
582 <https://doi.org/10.1016/j.rser.2021.111317>.

583 Calfapietra C., Fares S., Manes F., Morani A., Sgrigna G., Loreto F., 2013. Role of Biogenic Volatile
584 Organic Compounds (BVOC) emitted by urban trees on ozone concentration in cities: A review.
585 *Environmental pollution (Barking, Essex 1987)* 183,71–80.
586 <https://doi.org/10.1016/j.envpol.2013.03.012>.

587 Caser M., Chitarra W., D'Angiolillo F., Perrone I., Demasi S., Lovisolo C., Pistelli L., Pistelli L., Scariot
588 V., 2019. Drought stress adaptation modulates plant secondary metabolite production in
589 *Salvia dolomitica* Codd. *Industrial Crops and Products* 129,85–96.
590 <https://doi.org/10.1016/j.indcrop.2018.11.068>.

591 Curci G., Beekmann M., Vautard R., Smiątek G., Steinbrecher R., Theloke J., Friedrich R., 2009.
592 Modelling study of the impact of isoprene and terpene biogenic emissions on European ozone
593 levels. *Atmospheric Environment* 43(7),1444–1455.
594 <https://doi.org/10.1016/j.atmosenv.2008.02.070>.

595 Dayan C., Fredj E., Misztal P.K., Gabay M., Guenther A.B., Tas E., 2020. Emission of biogenic volatile
596 organic compounds from warm and oligotrophic seawater in the Eastern Mediterranean.
597 *Atmos. Chem. Phys.* 20(21),12741–12759. <https://doi.org/10.5194/acp-20-12741-2020>.

598 Duhl T.R., Helmig D., Guenther A., 2008. Sesquiterpene emissions from vegetation: A review.
599 *Biogeosciences* 5(3),761–777. <https://doi.org/10.5194/bg-5-761-2008>.

600 Filella I., Primante C., Llusà J., Martín González A.M., Seco R., Farré-Armengol G., Rodrigo A.,
601 Bosch J., Peñuelas J., 2013. Floral advertisement scent in a changing plant-pollinators market.
602 *Scientific reports* 3,3434. <https://doi.org/10.1038/srep03434>.

603 Fitzky A.C., Kaser L., Peron A., Karl T., Graus M., Tholen D., Halbwirth H., Trimmel H., Pesendorfer
604 M., Rewald B., Sandén H., 2023. Same, same, but different: Drought and salinity affect BVOC
605 emission rate and alter blend composition of urban trees. *Urban Forestry & Urban Greening*
606 80(7),127842. <https://doi.org/10.1016/j.ufug.2023.127842>.

607 Fortunati A., Barta C., Brilli F., Centritto M., Zimmer I., Schnitzler J.-P., Loreto F., 2008. Isoprene
608 emission is not temperature-dependent during and after severe drought-stress: A
609 physiological and biochemical analysis. *The Plant journal for cell and molecular biology*
610 55(4),687–697. <https://doi.org/10.1111/j.1365-313X.2008.03538.x>.

611 Genard-Zielinski A.-C., Boissard C., Fernandez C., Kalogridis C., Lathière J., Gros V., Bonnaire N.,
612 Ormeño E., 2015. Variability of BVOC emissions from a Mediterranean mixed forest in
613 southern France with a focus on *Quercus pubescens*. *Atmos. Chem. Phys.*
614 15(1),431–446. <https://doi.org/10.5194/acp-15-431-2015>.

615 Genard-Zielinski A.-C., Boissard C., Ormeño E., Lathière J., Reiter I.M., Wortham H., Orts J.-P.,
616 Temime-Roussel B., Guenet B., Bartsch S., Gauquelin T., Fernandez C., 2018. Seasonal
617 variations of *Quercus pubescens*; isoprene emissions from an *in*
618 *natura* forest under drought stress and sensitivity to future climate change in the

619 Mediterranean area. *Biogeosciences* 15(15),4711–4730. [https://doi.org/10.5194/bg-15-](https://doi.org/10.5194/bg-15-4711-2018)
620 4711-2018.

621 Geron C., Daly R., Harley P., Rasmussen R., Seco R., Guenther A., Karl T., Gu L., 2016. Large
622 drought-induced variations in oak leaf volatile organic compound emissions during PINOT
623 NOIR 2012. *Chemosphere* 146,8–21. <https://doi.org/10.1016/j.chemosphere.2015.11.086>.

624 Giorgi F., Lionello P., 2008. Climate change projections for the Mediterranean region. *Global and*
625 *Planetary Change* 63(2-3),90–104. <https://doi.org/10.1016/j.gloplacha.2007.09.005>.

626 Goldstein A.H., McKay M., Kurpius M.R., Schade G.W., Lee A., Holzinger R., Rasmussen R.A., 2004.
627 Forest thinning experiment confirms ozone deposition to forest canopy is dominated by
628 reaction with biogenic VOCs. *Geophys. Res. Lett.* 31(22),22,123.
629 <https://doi.org/10.1029/2004GL021259>.

630 Greenberg J.P., Asensio D., Turnipseed A., Guenther A.B., Karl T., Gochis D., 2012. Contribution of
631 leaf and needle litter to whole ecosystem BVOC fluxes. *Atmospheric Environment* 59,302–311.
632 <https://doi.org/10.1016/j.atmosenv.2012.04.038>.

633 Guenther A., 2013. Biological and Chemical Diversity of Biogenic Volatile Organic Emissions into
634 the Atmosphere. *ISRN Atmospheric Sciences* 2013(19),1–27.
635 <https://doi.org/10.1155/2013/786290>.

636 Guenther A., Hewitt C.N., Erickson D., Fall R., Geron C., Graedel T., Harley P., Klinger L., Lerdau M.,
637 McKay W.A., Pierce T., Scholes B., Steinbrecher R., Tallamraju R., Taylor J., Zimmerman P.,
638 1995. A global model of natural volatile organic compound emissions. *J. Geophys. Res.*
639 100(D5),8873–8892.

640 Guenther A.B., Jiang X., Heald C.L., Sakulyanontvittaya T., Duhl T., Emmons L.K., Wang X., 2012.
641 The Model of Emissions of Gases and Aerosols from Nature version 2.1 (MEGAN2.1): An
642 extended and updated framework for modeling biogenic emissions. *Geosci. Model Dev.*
643 5(6),1471–1492. <https://doi.org/10.5194/gmd-5-1471-2012>.

644 Han Z., Zhang Y., Zhang H., Ge X., Gu D., Liu X., Bai J., Ma Z., Tan Y., Zhu F., Xia S., Du J., Tan Y., Shu
645 X., Tang J., Sun Y., 2022. Impacts of Drought and Rehydration Cycles on Isoprene Emissions in
646 *Populus nigra* Seedlings. *International journal of environmental research and public health*
647 19(21). <https://doi.org/10.3390/ijerph192114528>.

648 Holopainen J.K., Gershenzon J., 2010. Multiple stress factors and the emission of plant VOCs.
649 *Trends in plant science* 15(3),176–184. <https://doi.org/10.1016/j.tplants.2010.01.006>.

650 Jiang X., Guenther A., Potosnak M., Geron C., Seco R., Karl T., Kim S., Gu L., Pallardy S., 2018.
651 Isoprene Emission Response to Drought and the Impact on Global Atmospheric Chemistry.
652 *Atmospheric environment* (Oxford, England 1994) 183,69–83.
653 <https://doi.org/10.1016/j.atmosenv.2018.01.026>.

654 Kesselmeier J., Staudt M., 1999. Biogenic Volatile Organic Compounds (VOC): An Overview on
655 Emission, Physiology and Ecology. *Journal of Atmospheric Chemistry* 33,23–88.

656 Li Q., Gabay M., Dayan C., Misztal P., Guenther A., Fredj E., Tas E., 2024. Instantaneous intraday
657 changes in key meteorological parameters as a proxy for the mixing ratio of BVOCs over
658 vegetation under drought conditions. *Atmos. Chem. Phys.*

659 Li Q., Gabay M., Rubin Y., Fredj E., Tas E., 2018. Measurement-based investigation of ozone
660 deposition to vegetation under the effects of coastal and photochemical air pollution in the

661 Eastern Mediterranean. *Science of The Total Environment* 645,1579–1597.
662 <https://doi.org/10.1016/j.scitotenv.2018.07.037>.

663 Lionello P., 2012. *The Climate of the Mediterranean Region: From the Past to the Future*: Elsevier.

664 Llusia J., Roahtyn S., Yakir D., Rotenberg E., Seco R., Guenther A., Peñuelas J., 2016. Photosynthesis,
665 stomatal conductance and terpene emission response to water availability in dry and mesic
666 Mediterranean forests. *Trees* 30(3),749–759. <https://doi.org/10.1007/s00468-015-1317-x>.

667 Llusia J., Peñuelas J., 2000. Seasonal patterns of terpene content and emission from seven
668 Mediterranean woody species in field conditions. *American J of Botany* 87(1),133–140.
669 <https://doi.org/10.2307/2656691>.

670 Medrano H., Escalona J.M., Bota J., Gulías J., Flexas J., 2002. Regulation of photosynthesis of C3
671 plants in response to progressive drought: Stomatal conductance as a reference parameter.
672 *Annals of botany* 89 Spec No(7),895–905. <https://doi.org/10.1093/aob/mcf079>.

673 MIYASHITA K., TANAKAMARU S., MAITANI T., KIMURA K., 2005. Recovery responses of
674 photosynthesis, transpiration, and stomatal conductance in kidney bean following drought
675 stress. *Environmental and Experimental Botany* 53(2),205–214.
676 <https://doi.org/10.1016/j.envexpbot.2004.03.015>.

677 Monson R.K., Jaeger C.H., Adams W.W., Driggers E.M., Silver G.M., Fall R., 1992. Relationships
678 among Isoprene Emission Rate, Photosynthesis, and Isoprene Synthase Activity as Influenced
679 by Temperature. *PLANT PHYSIOLOGY* 98(3),1175–1180.

680 Niinemets U., Loreto F., Reichstein M., 2004. Physiological and physicochemical controls on foliar
681 volatile organic compound emissions. *Trends in plant science* 9(4),180–186.
682 <https://doi.org/10.1016/j.tplants.2004.02.006>.

683 Niinemets U., Monson R.K., 2013. *Biology, controls and models of tree volatile organic compound*
684 *emissions*. Dordrecht: Springer.

685 Nobel P.S., 1999. *Physicochemical & environmental plant physiology*. 2nd ed. San Diego:
686 Academic Press.

687 Núñez L., Plaza J., Pérez-Pastor R., Pujadas M., Gimeno B.S., Bermejo V., García-Alonso S., 2002.
688 High water vapour pressure deficit influence on *Quercus ilex* and *Pinus pinea* field
689 monoterpene emission in the central Iberian Peninsula (Spain). *Atmospheric Environment*
690 36(28),4441–4452. [https://doi.org/10.1016/S1352-2310\(02\)00415-6](https://doi.org/10.1016/S1352-2310(02)00415-6).

691 Owen S., Boissard C., Street R.A., Duckham S.C., Csiky O., Hewitt C.N., 1997. Screening of 18
692 Mediterranean plant species for volatile organic compound emissions. *Atmospheric*
693 *Environment* 31,101–117. [https://doi.org/10.1016/S1352-2310\(97\)00078-2](https://doi.org/10.1016/S1352-2310(97)00078-2).

694 Owen S.M., Hewitt C.N., 2000. Extrapolating branch enclosure measurements to estimates of
695 regional scale biogenic VOC fluxes in the northwestern Mediterranean basin. *J. Geophys. Res.*
696 105(D9),11573–11583. <https://doi.org/10.1029/1999JD901154>.

697 Pegoraro E., REY A.N.A., Abrell L., van HAREN J., LIN G., 2006. Drought effect on isoprene
698 production and consumption in Biosphere 2 tropical rainforest. *Glob Change Biol* 12(3),456–
699 469. <https://doi.org/10.1111/j.1365-2486.2006.01112.x>.

700 Peñuelas J., Munné-Bosch S., 2005. Isoprenoids: An evolutionary pool for photoprotection. *Trends*
701 *in plant science* 10(4),166–169. <https://doi.org/10.1016/j.tplants.2005.02.005>.

702 Peñuelas J., Rutishauser T., Filella I., 2009. Ecology. Phenology feedbacks on climate change.
703 Science (New York, N.Y.) 324(5929),887–888. <https://doi.org/10.1126/science.1173004>.

704 Peñuelas J., Staudt M., 2010. BVOCs and global change. Trends in plant science 15(3),133–144.
705 <https://doi.org/10.1016/j.tplants.2009.12.005>.

706 Potosnak M.J., LeSturgeon L., Pallardy S.G., Hosman K.P., Gu L., Karl T., Geron C., Guenther A.B.,
707 2014. Observed and modeled ecosystem isoprene fluxes from an oak-dominated temperate
708 forest and the influence of drought stress. Atmospheric Environment 84,314–322.
709 <https://doi.org/10.1016/j.atmosenv.2013.11.055>.

710 Ryan A.C., Hewitt C.N., Possell M., Vickers C.E., Purnell A., Mullineaux P.M., Davies W.J., Dodd I.C.,
711 2014. Isoprene emission protects photosynthesis but reduces plant productivity during
712 drought in transgenic tobacco (*Nicotiana tabacum*) plants. New Phytol 201(1),205–216.
713 <https://doi.org/10.1111/nph.12477>.

714 Saunders S.M., Jenkin M.E., Derwent R.G., Pilling M.J., 2003. Protocol for the development of the
715 Master Chemical Mechanism, MCM v3 (Part A): tropospheric degradation of non-aromatic
716 volatile organic compounds. Atmos. Chem. Phys. 3,161–180.

717 Saunier A., Ormeño E., Boissard C., Wortham H., Temime-Roussel B., Lecareux C., Armengaud A.,
718 Fernandez C., 2017. Effect of mid-term drought on *Quercus pubescens*
719 BVOCs' emission seasonality and their dependency on light and/or temperature. Atmos. Chem.
720 Phys. 17(12),7555–7566. <https://doi.org/10.5194/acp-17-7555-2017>.

721 Schade G.W., Goldstein A.H., Lamanna M.S., 1999. Are monoterpene emissions influenced by
722 humidity? Geophys. Res. Lett. 26(14),2187–2190.

723 Seco R., Karl T., Turnipseed A., Greenberg J., Guenther A., Llusia J., Peñuelas J., Dicken U.,
724 Rotenberg E., Kim S., Yakir D., 2017. Springtime ecosystem-scale monoterpene fluxes from
725 Mediterranean pine forests across a precipitation gradient. Agricultural and Forest
726 Meteorology 237-238,150–159. <https://doi.org/10.1016/j.agrformet.2017.02.007>.

727 Sindelarova K., Granier C., Bouarar I., Guenther A., Tilmes S., Stavrakou T., Müller J.-F., Kuhn U.,
728 Stefani P., Knorr W., 2014. Global data set of biogenic VOC emissions calculated by the MEGAN
729 model over the last 30 years. Atmos. Chem. Phys. 14(17),9317–9341.
730 <https://doi.org/10.5194/acp-14-9317-2014>.

731 Staudt M., Mandl N., Joffre R., Rambal S., 2001. Intraspecific variability of monoterpene
732 composition emitted by *Quercus ilex* leaves. Can. J. For. Res. 31(1),174–180.
733 <https://doi.org/10.1139/x00-153>.

734 Street R.A., Owen S., Duckham S.C., Boissard C., Hewitt C.N., 1997. Effect of habitat and age on
735 variations in volatile organic compound (VOC) emissions from *Quercus ilex* and *Pinus pinea*.
736 Atmospheric Environment 31,89–100. [https://doi.org/10.1016/S1352-2310\(97\)00077-0](https://doi.org/10.1016/S1352-2310(97)00077-0).

737 Tingey D., Turner D., Weber J., 1990. Factors Controlling the Emissions of Monoterpenes and
738 Other Volatile Organic Compounds: U.S. Environmental Protection Agency, Washington, D.C.
739 EPA/600/D-90/195 (NTIS PB91136622).

740 Vilagrosa A., Bellot J., Vallejo V.R., Gil-Pelegrin E., 2003. Cavitation, stomatal conductance, and
741 leaf dieback in seedlings of two co-occurring Mediterranean shrubs during an intense drought.
742 Journal of experimental botany 54(390),2015–2024. <https://doi.org/10.1093/jxb/erg221>.

743